SUPPLEMENTAL MATERIAL

1. **Supplemental Figure Legends**
2. **Supplemental Figures 1-9**
3. **Supplemental Tables 1-2**

Supplemental Figure 1. SA2 is frequently mutated in EWS and BUC. (**A, B**) Genomic alterations of *SA1*, *SA2* and *SA3* in NCI-60 cell lines (**A**) and in the MSK-IMPACT dataset (**B**). (**C, D**) Representative immunohistochecmical images of SA1 and SA2 expression in human bladder cancer samples (n = 169). SA1 expression is quantified as low-to-high staining (**C**), whereas SA2 mutation is determined as no staining in tumor cells in contrast to positive staining in stroma cells (**D**). (**E-G**) Protein levels of SA3 is in human EWS (**E**) and BUC (**F**) cell lines and tissue samples (**G**). Scale bar, 50 μm. Data are representative of three independent experiments.

Supplemental Figure 2. Depletion of SA1 leads to synthetic lethality in SA2-mutated cancer cells. (**A, B**) SA1 expression levels (determined by Western blot) in EWS (**A**) and BUC (**B**) cell lines expressing control (shNT) or SA1-specific shRNAs (shSA1). (**C**) Effect of SA1 knockdown on the proliferation of the SA2-intact RT4 and the SA2-mutate UC3 cells, determined by direct competition assay. Cells expressing RFP and shNT or shSA1 were sorted and mixed with control RFP-negative cells (1:1) and the RFP-positive cells were quantified at passages 2, 4 and 6. (**D, E**) Cell survival (**D**, measured by crystal violet staining) and protein expression levels (**E,** measured by wester blotting) of SA1 and SA2 in TC32 and UC3 cells expressing shSA1, control or ectopic SA2. ** $p < 0.01$ by one-way ANOVA with Tukey's t test. Data are presented as the mean ± SD and are representative of three independent experiments.

Supplemental Figure 3. Truncating mutation of *SA2* sensitizes SA2-intact cells to SA1 depletion. (**A**) Truncating mutation profile of *SA2* in EWS and BUC. R216* and Q593* are the top 2 mutation sites identified in cancer patients. (**B**) Schematic illustration of the Cas9/sgRNA-targeting sites in the *SA2* gene. Two single-guide RNA (sgRNA)-targeting sequences are shown and the protospacer-adjacent motif (PAM) sequences are highlighted in red. (**C**) Sequences of

mutant SA2 allele in the cell colonies (#1 and #2) for TC71 or RT4 cell line. PAM sequences are highlighted in red. Small deletions in the targeted region led to open reading frame shift, producing only a short stretch of the amino-terminal peptide without any functional SA2. (**D, E**) SA2 protein levels (**D**) and growth curves (**E**) of parental and the SA2-mutated TC71 and RT4 cells. (**F, G**) Dox-induced suppression of SA1 by shSA1 #1 or shSA1 #3 inhibited the growth of the SA2-mutated cells, but not of their parental TC71 and RT4 cells (**F**). Knockdown efficiency of SA1 was shown in (**G**). One-way ANOVA followed by Tukey's t test were conducted to determine statistical significance between indicated groups. Data are presented as the mean ± SD and are representative of three independent experiments.

Supplemental Figure 4. Knockdown of SA1 inhibits the growth of SA2-mutated tumors *in vivo*. (**A**) Representative images of H&E, SA1, Ki-67 (cell proliferation) and cleaved caspase-3 (apoptosis) staining in orthotopically implanted TC71 and TC32 Ewing sarcoma tissues. (**B**) Representative images of H&E, SA1, Ki-67 (cell proliferation) and cleaved caspase-3 (apoptosis) staining in subcutaneously implanted RT4 and UC3 bladder urothelial tumor tissues. (**C-E**) Quantification of SA1, Ki-67 (cell proliferation) or cleaved caspase-3 (apoptosis) staining in the aforementioned tumor tissues. n = 5 mice per group. (**F**) Representative protein levels of SA1 in the above xenograft tumors with or without Dox-induced SA1 knockdown. ** $p<0.01$ and *** $p<0.001$ versus control by unpaired two-tailed t-test. Data are presented as the mean ± SD and are representative of three independent experiments.

Supplemental Figure 5. Depletion of SA1 in primary mesenchymal stem cell (MSC) has no or modest effect on chromosome alignment and segregation. (**A, B**) Representative metaphase images (**A**) and quantification of cohesion defects (**B**) in MSC cells expressing Dox-

induced non-specific control shNT or SA1-specific shSA1. (**C**) Knockdown efficiency of SA1-specific shRNAs in the MSC cells described above. (**D**, **E**) Quantitative PCR (**D**) and western blot (**E**) analysis of SA1 shRNA knockdown efficiency in TC71 and TC32 Ewing sarcoma cell lines with or without Dox-induced SA1 knockdown. Fisher's exact test were conducted to determine statistical significance between indicated groups in (**B**). Data are presented as the mean ± SD and are representative of three independent experiments.

Supplemental Figure 6. SA2-mutated cells, upon depletion of SA1, are defective in DSB DNA repair. (**A**) Quantification of HRD scores in TC71 and TC32 cells with or without Dox-induced knockdown of SA1. HRD score is determined by the correlation to the HRD gene signature, and higher scores are more likely to have HR defects. (**B**) Up-regulation of CDKN1c and down-regulation of BLM, BRCA1, CHEK1, DNA2 and FANCI expression in the SA2-mutated cells with SA1 knockdown. The RNA expression levels were determined by quantitative PCR. (**C**) Knockdown efficiency of SA1-specific siRNAs in TC71, TC32, RT4 and UC3 cancer cells. (**D**) Micrographs of parental and the isogenic SA2-mutated TC71 cells with or without SA1 knockdown. Cells were stained for γ-H2AX at indicated time points following 5 Gy of IR treatment. The histograms show the number of γ-H2AX per cell. * $p<0.05$, ** $p<0.01$ and *** $p<0.001$ versus control by unpaired two-tailed t-test. Data are presented as the mean ± SD and are representative of three independent experiments.

Supplemental Figure 7. Depletion of SA1 in primary mesenchymal stem cells (MSCs) does not affect their sensitivity to PARP inhibitors. (**A**) Fraction of apoptotic cells (Annexin V positive) in the parental or SA2-mutated TC71 or RT4 cells treated with SA1 knockdown and/or 10 μM Olaparib for 72 h. (**B**) Dose-dependent responses of the SA2-intact or -mutated cell lines

to the treatment of cisplatin (72h) with or without SA1 knockdown. (**C, D**) After transfection with control or SA1-specific siRNAs for 24 h, primary endothelial MSC cells were treated with the indicated PARP inhibitors for 72 h. Clonogenic assay was performed. The representative images are shown in (**C**) and the quantitative results are shown in the bar diagrams (**D**). (**E**) Western blot analyses showed the effective SA1 knockdown. (**F**) Quantification of cohesion defects in TC32 cells expressing Dox-induced control shRNA or shSA1 with or without BMN-673 (10 nM) treatment. (**G**) Percentages of mitotic fates in TC32 cells after combined treatment with Dox-induced SA1 knockdown and BMN-673 (10 nM). ** $p<0.01$ and *** $p<0.001$ versus control by unpaired two-tailed t-test (**A**) and Fisher's exact test (**F**, **G**). Data are presented as the mean ± SD and are representative of three independent experiments.

Supplemental Figure 8. Depletion of SA1 sensitizes SA2-mutated tumors to the treatment of PARP inhibitor BMN-673. (**A, B**) Representative images of H&E, SA1, Ki-67 (cell proliferation) and cleaved caspase-3 (apoptosis) staining in orthotopically implanted TC32 (**A**) and UC3 (**B**) tumor tissues. (**C, D**) Representative protein levels of SA1 in the above xenograft tumors after siSA1-DOPC or BMN-673 treatment. (**E, F**) Changes in the body weights of NU/J mice with treatments as described in TC32 (**E**, n =5) and UC3 groups (**F**, n =5). Data are representative of three independent experiments.

Supplemental Figure 9. Depletion of SA1 does not sensitize SA2-intact tumors to the treatment of PARP inhibitor BMN-673. (**A-F**) Tumor growth curves (**A, D**), representative bioluminescent images (**B, E**) and gross tumor weights (**C, F**) of xenograft tumors derived from orthotopically implanted TC71 (**A-C**) or RT4 (**D-F**) cells. Once tumor was established, mice were randomly divided to 4 groups and then treated with DMSO and siNT-DOPC, siSA1-DOPC

nanoliposome (twice weekly), BMN-673 (daily), or the combination of siSA1-DOPC nanoliposome and BMN-673. n = 5 mice per group. (**G, H**) Representative protein levels of SA1 in the above xenograft tumors after siSA1-DOPC nanoliposome or BMN-673 treatment. One-way ANOVA followed by Tukey's t test were conducted to determine statistical significance between indicated groups. Data are presented as the mean ± SD.

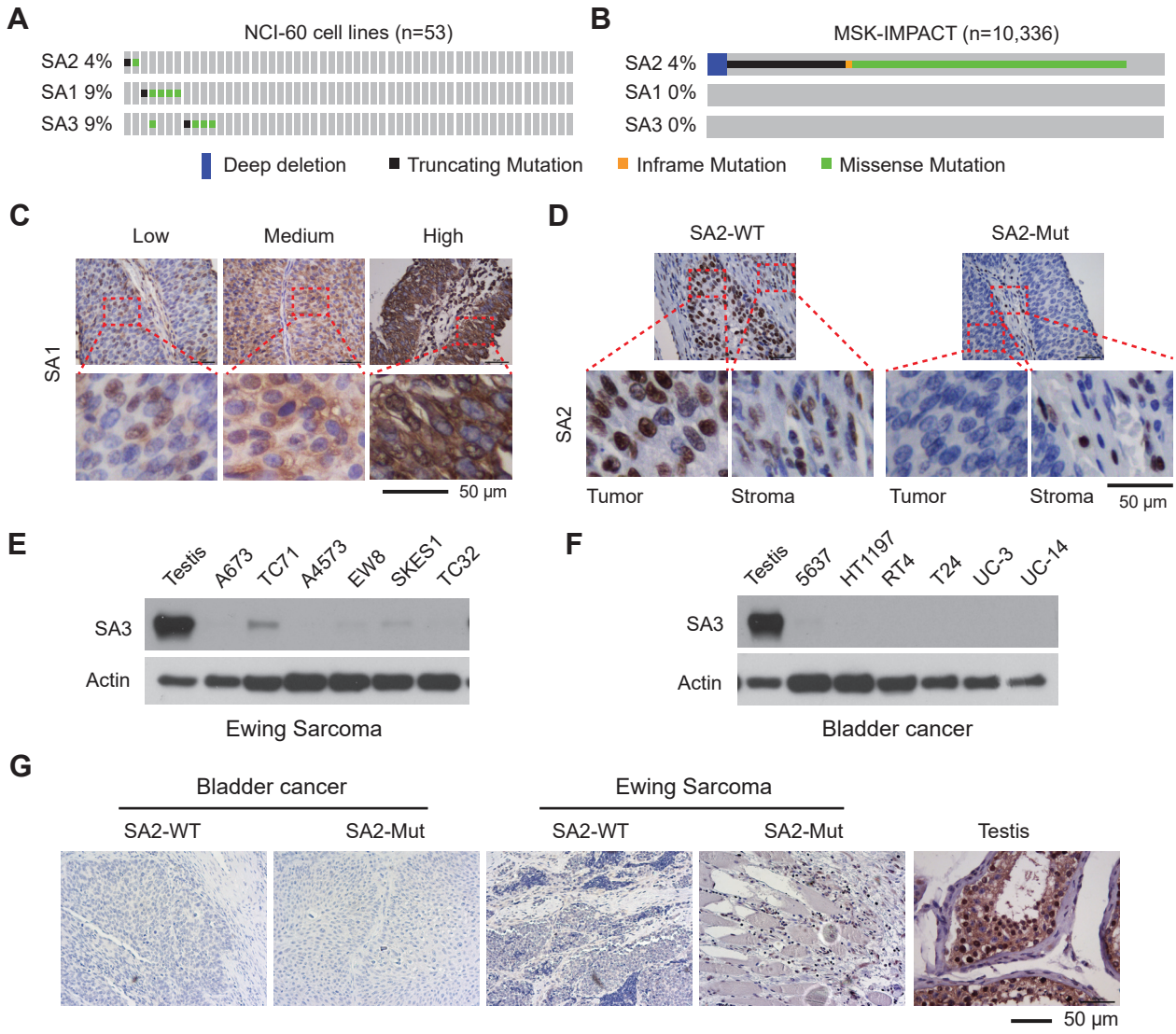

Supplemental Figure 1

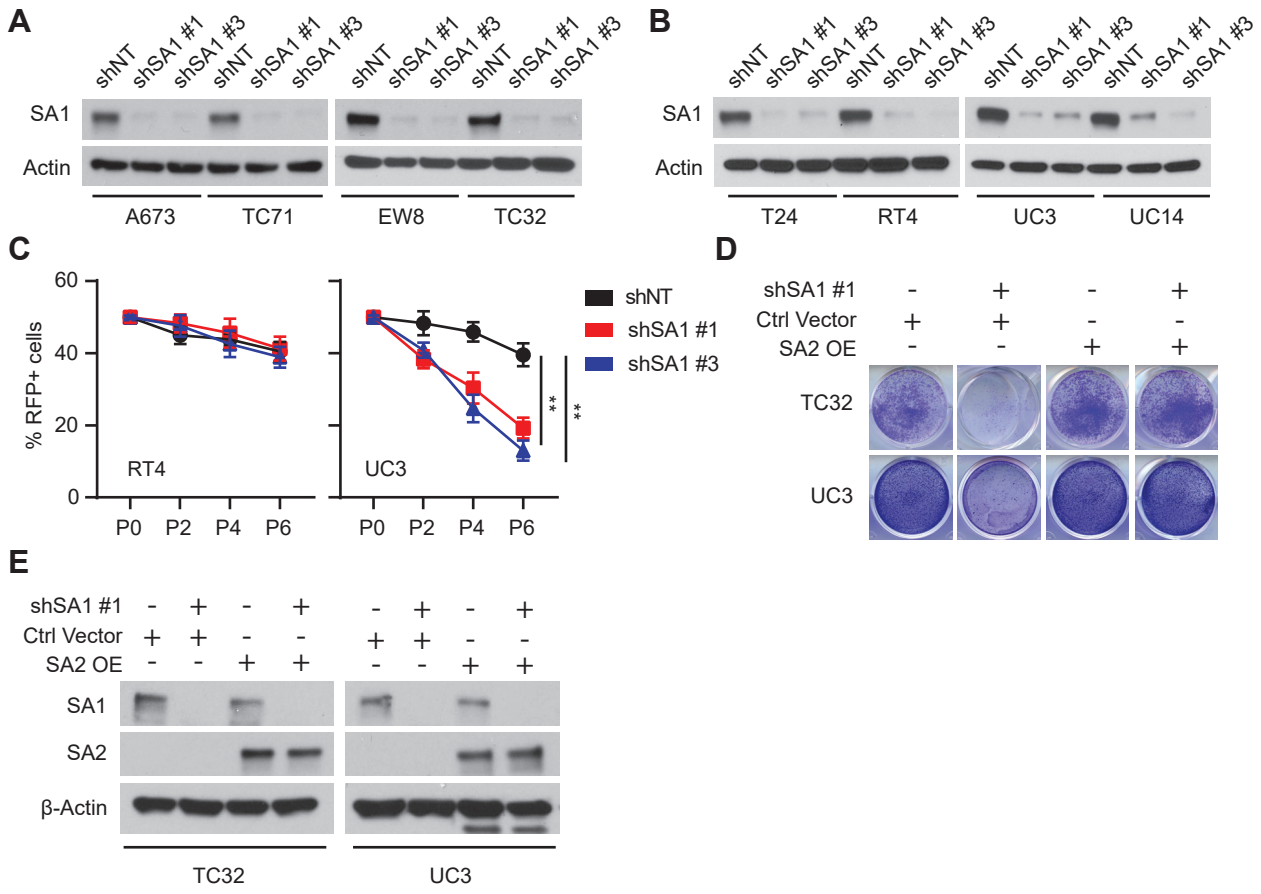

Supplemental Figure 2

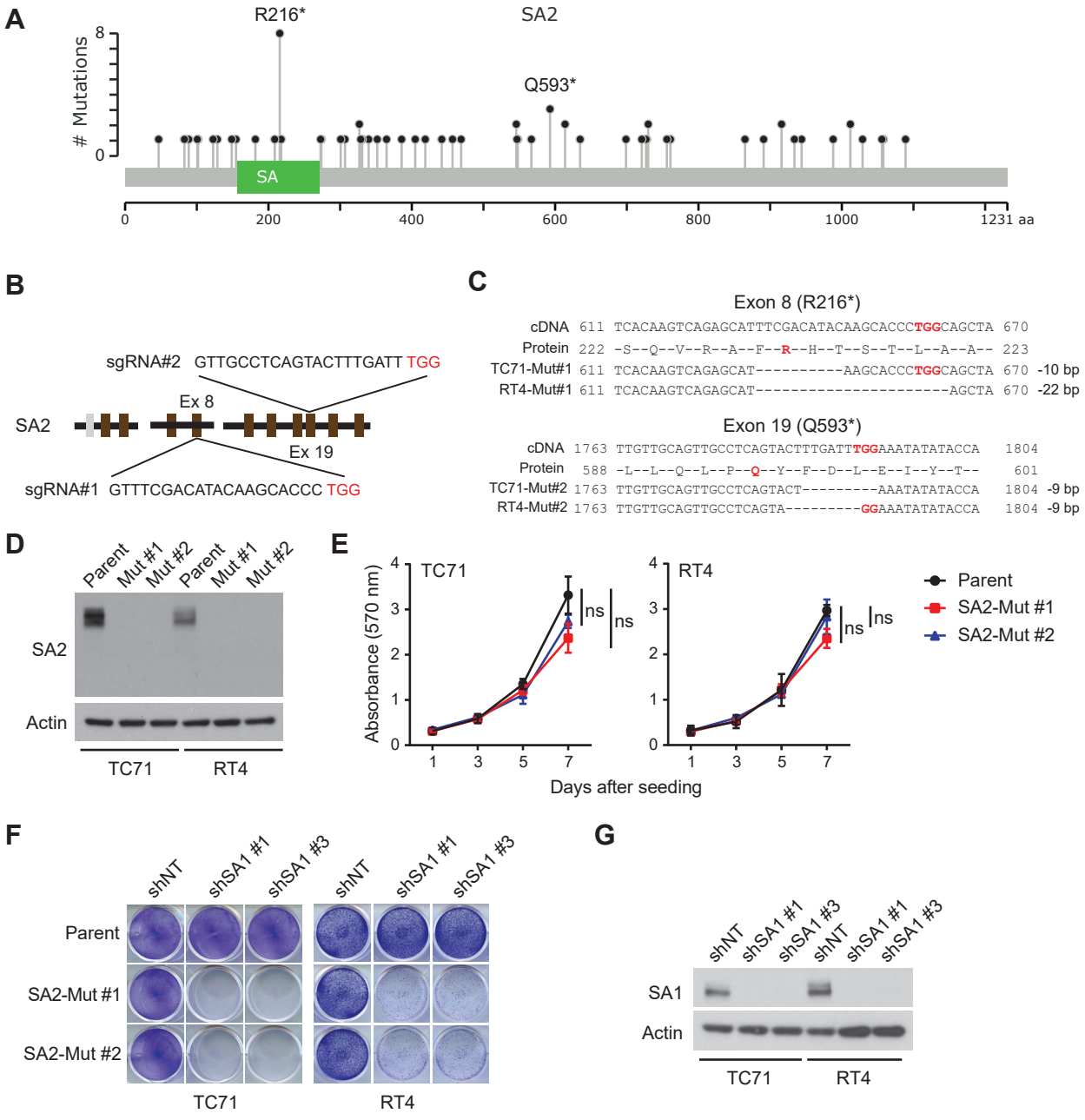

Supplemental Figure 3

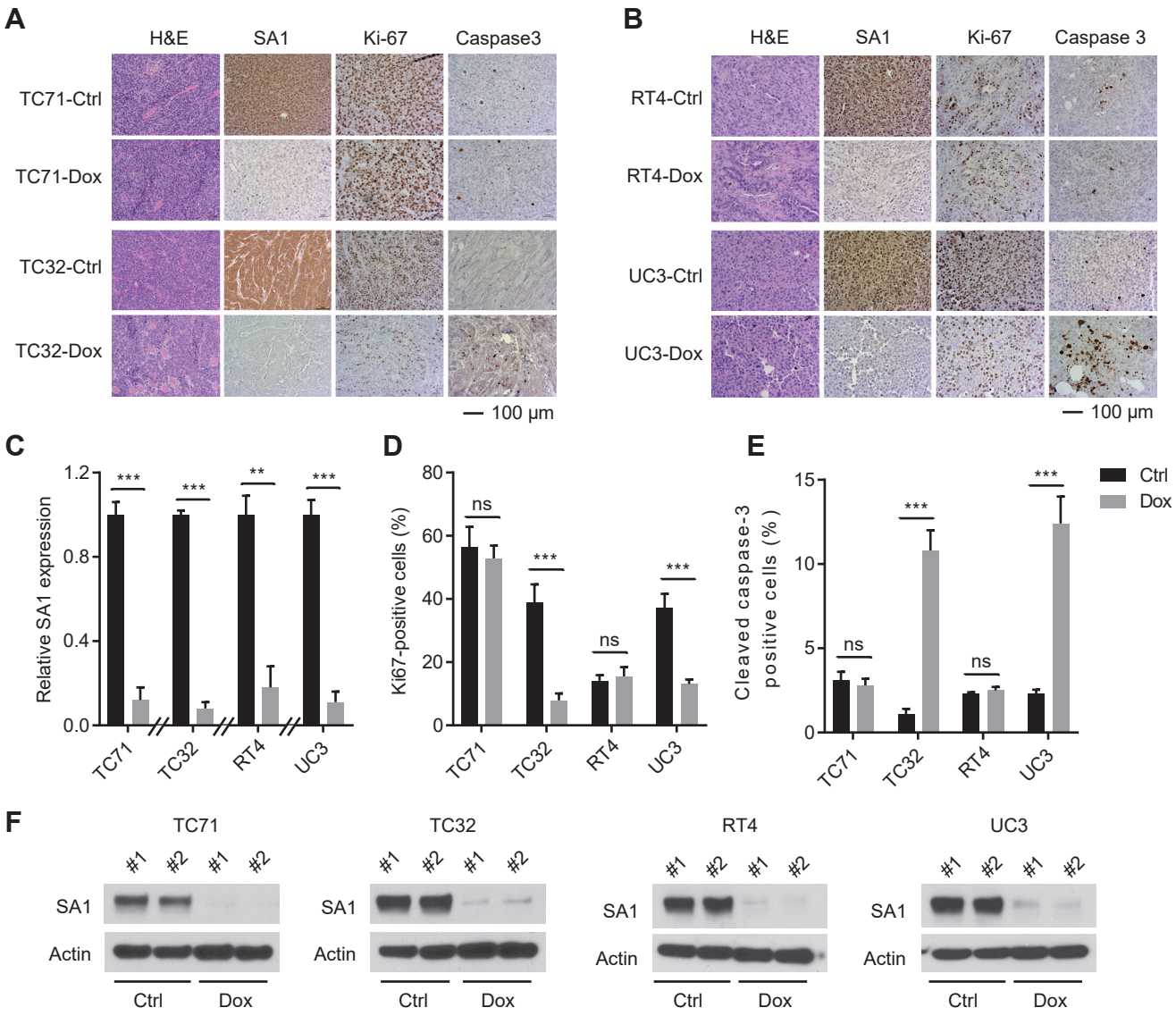

Supplemental Figure 4

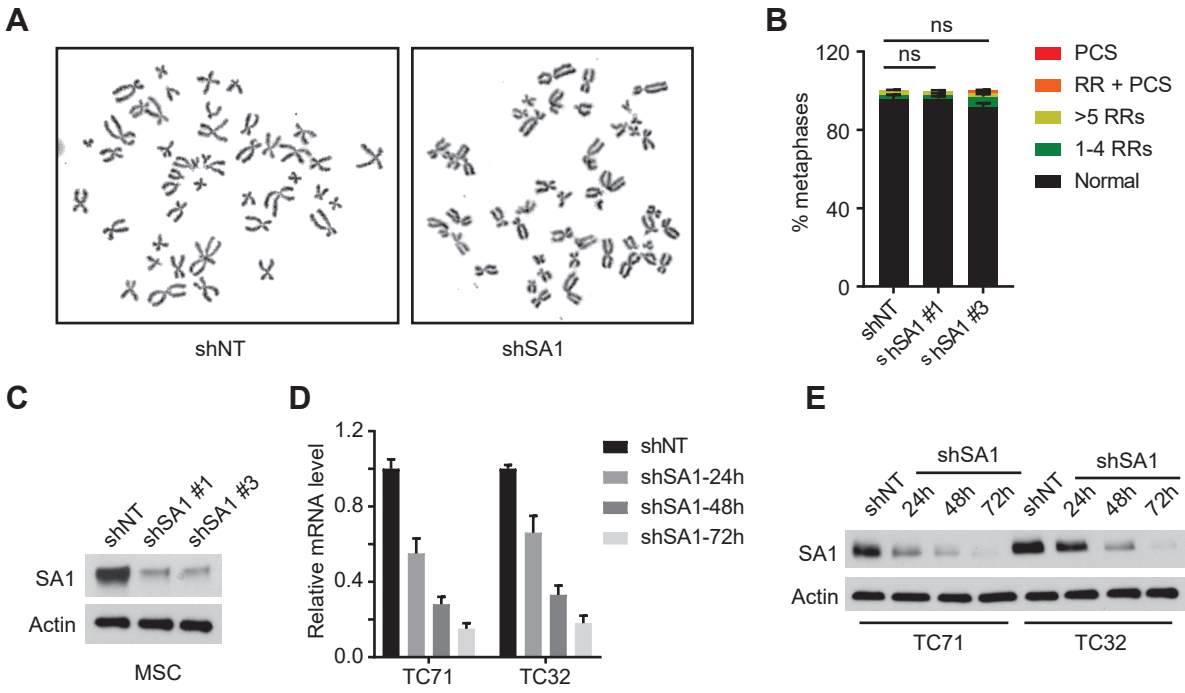

Supplemental Figure 5

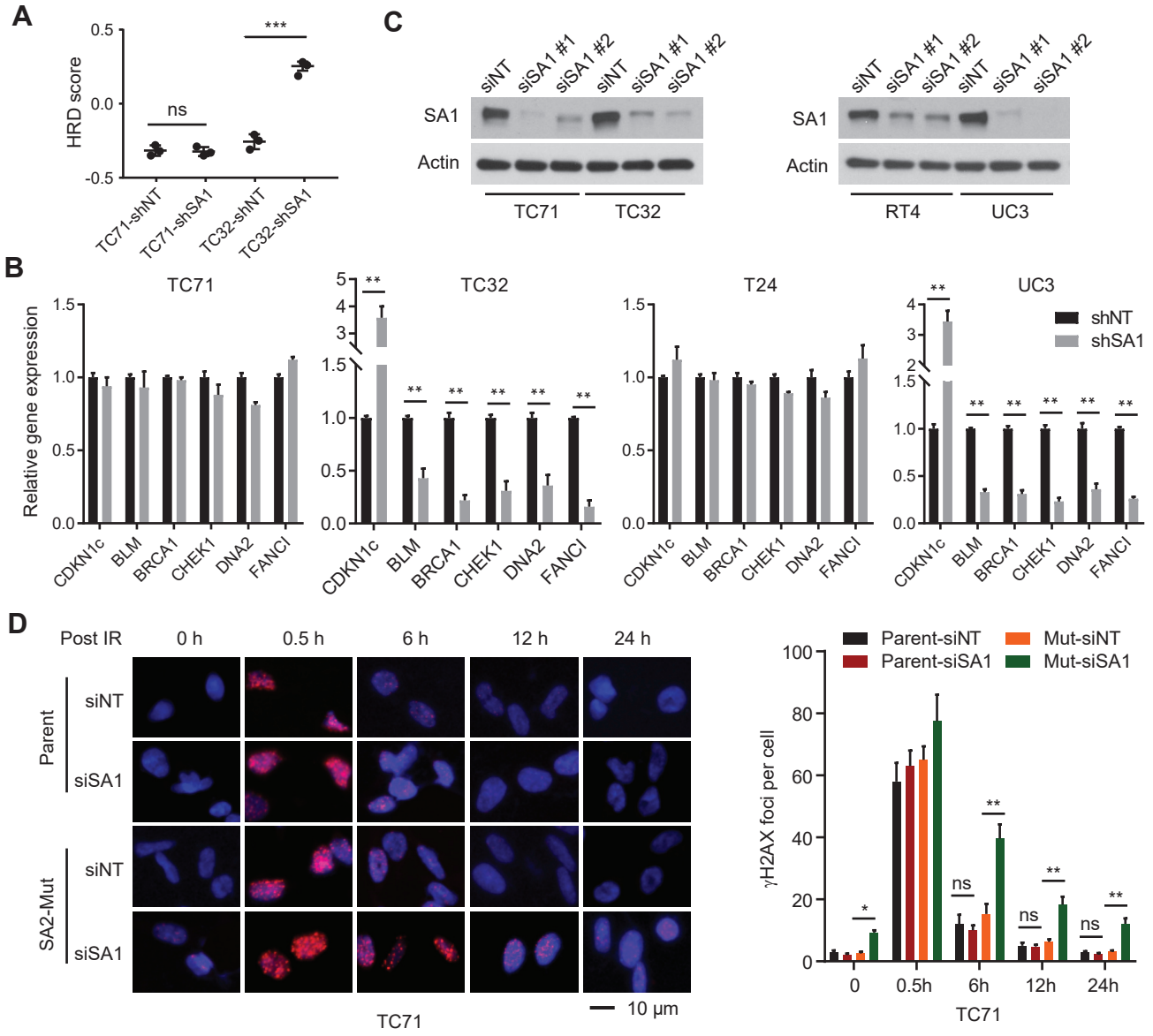

Supplemental Figure 6

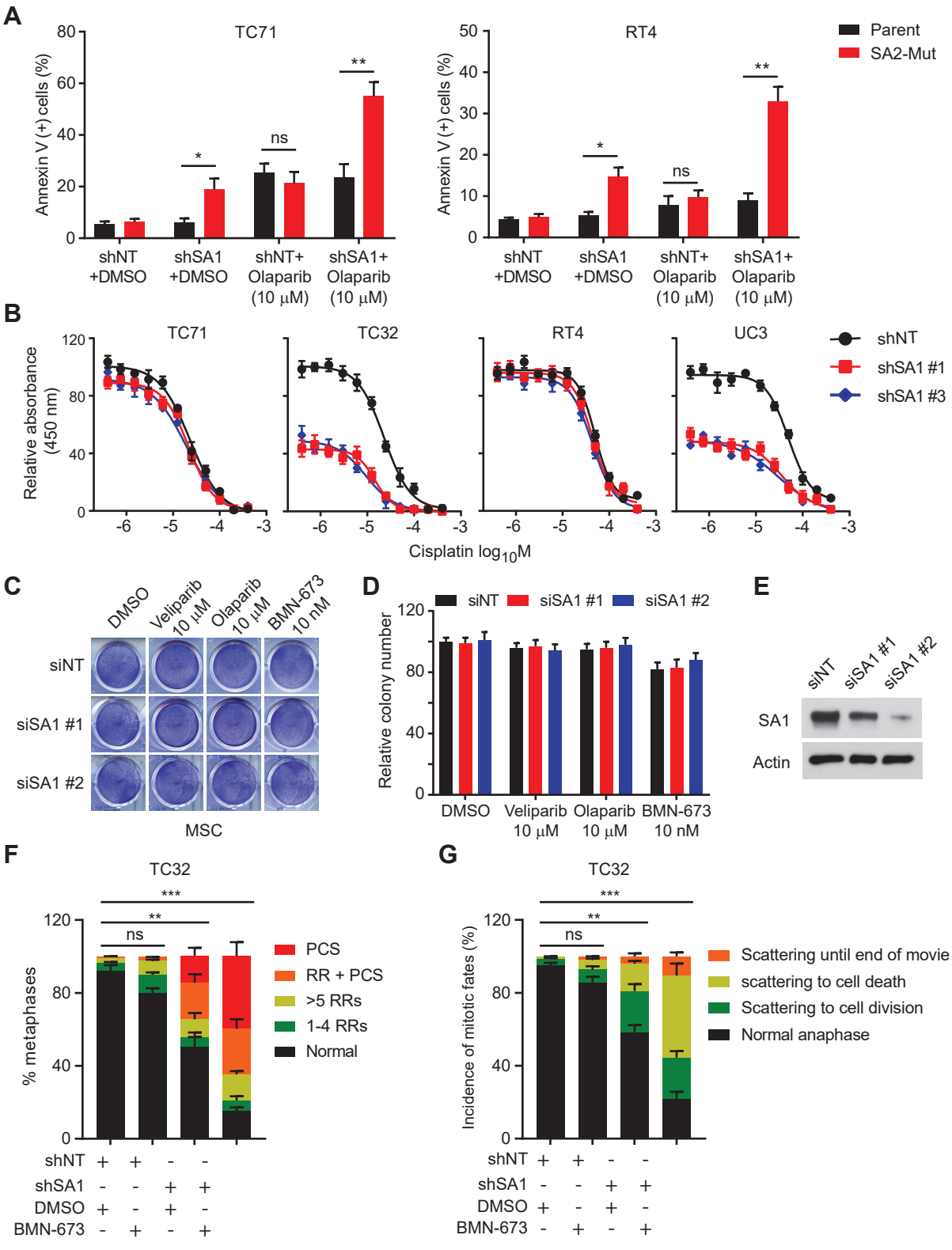

Supplemental Figure 7

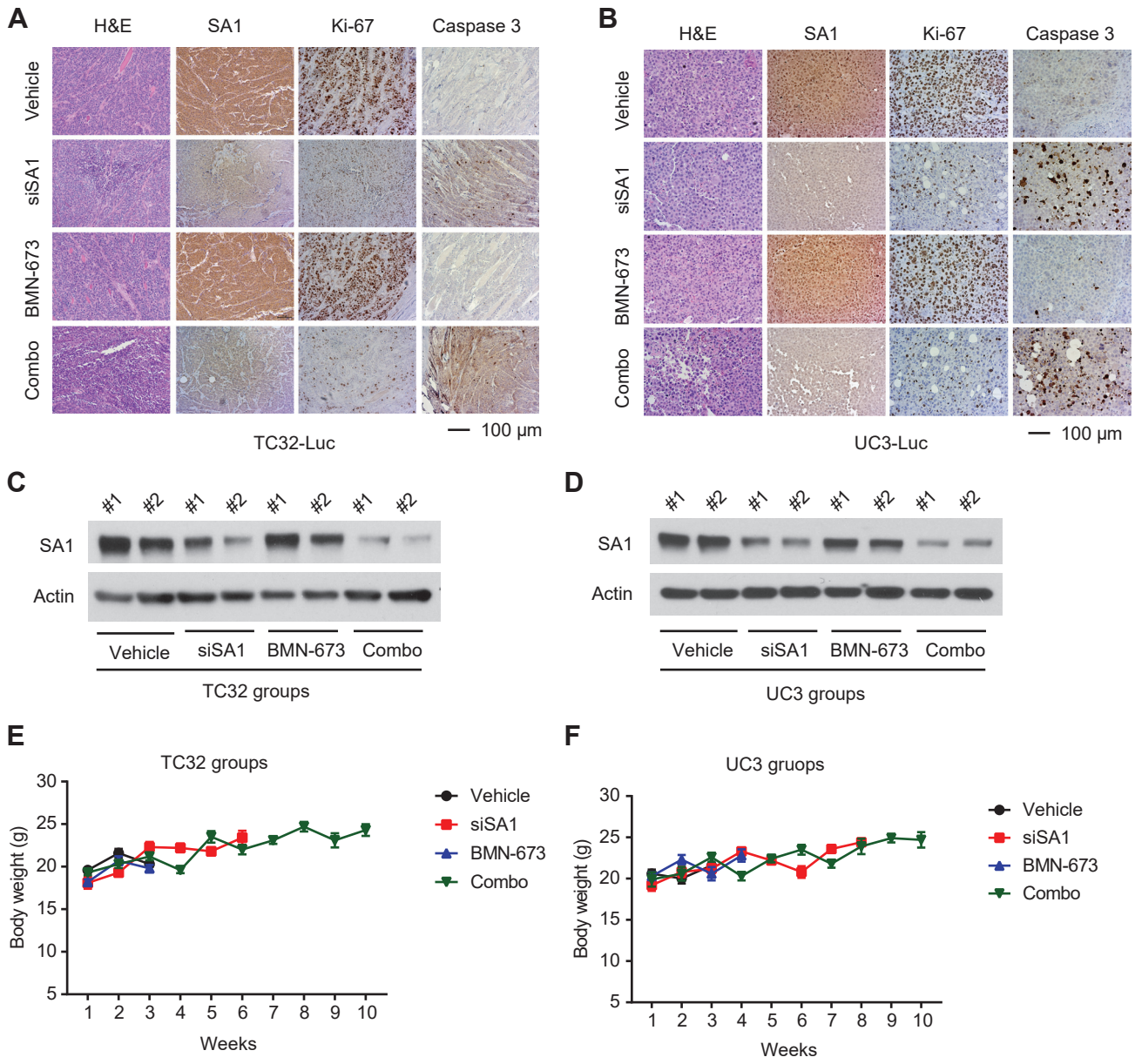

Supplemental Figure 8

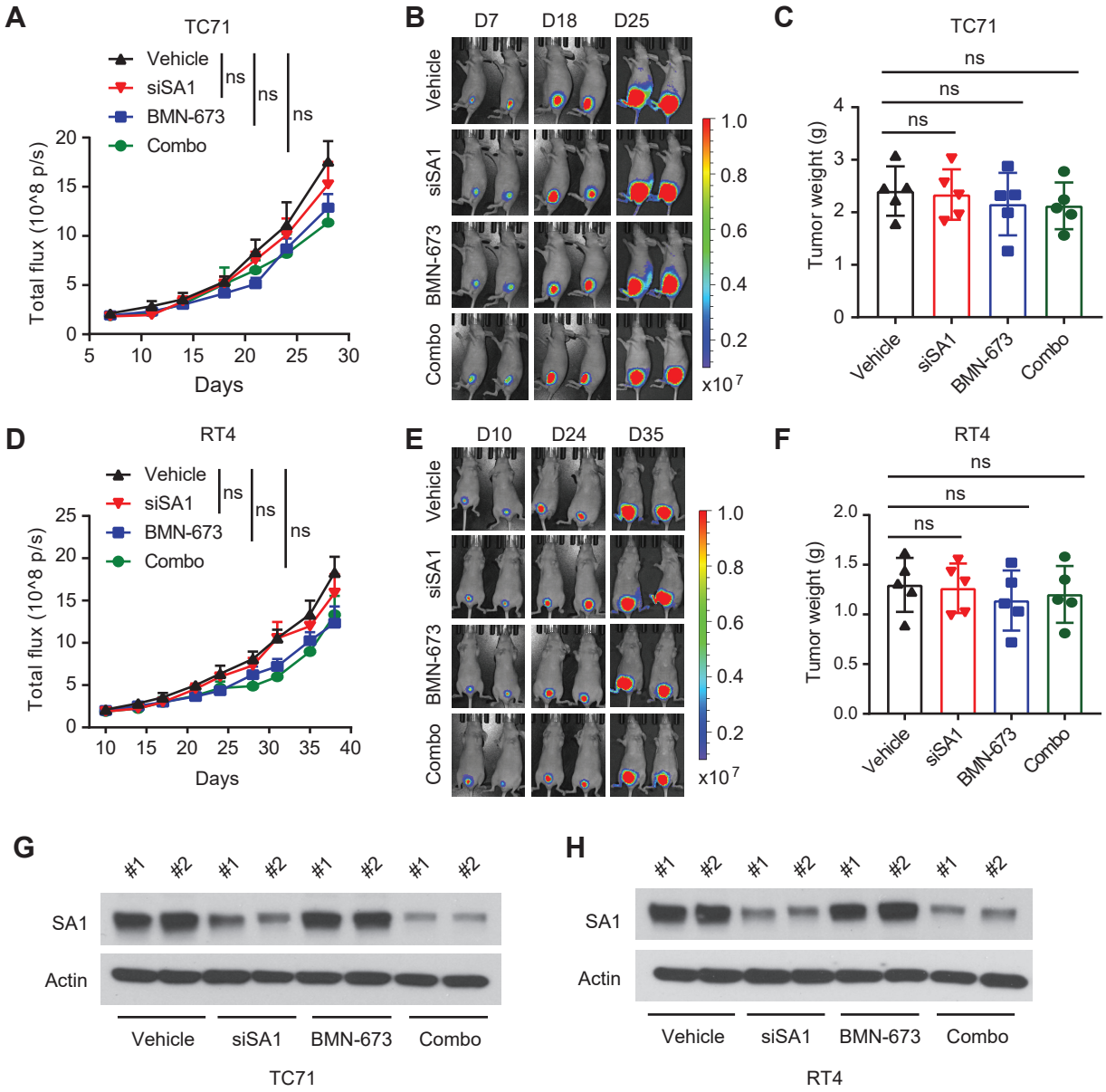

Supplemental Figure 9

Supplemental Table 1. Most frequently mutated essential redundant genes in human cancers.

Mutated gene	Chromosome locus	Mutation rate (%) in cancer	Target paralog	Pathway
KDM6A	Xp11.3	BLCA 26.5	KDM6B	Histone modifier
KDM5C	Xp11.22	KIRC 6.5	KDM5A/B	Histone modifier
SA2	Xq25	BLCA 15.0	SA1	Genome integrity
ARID1A	1p36.11	BLCA 27.6; UCEC 30.0	ARID1B	Histone modifier
BRG1	19p13.2	LUAD 12.0	BRM	Histone modifier
FOXA1	14q21.1	BLCA 4.1	FOXA2	Transcription factor
SMC1A	Xp11.22	UCEC 4.4	SMC1B	Genome integrity
CDKN1A	6p21.2	BLCA 12.2	CDKN1B	Cell cycle
NFE2L2	2q31.2	LUSC 14.9	NFE2L3	Nuclear factor
ACVR1B	12q13.13	COAD/READ 3.6	ACVR1A	TGF-beta signaling

UCEC: Uterine Corpus Endometrial Carcinoma; BLCA: Urothelial Bladder Carcinoma; KIRC: Kidney Renal Clear Cell Carcinoma; LUAD: Lung Adenocarcinoma; LUSC: Lung Squamous Cell Carcinoma.

Supplemental Table 2. Sequences of oligonucleotide primers.

Name	Sequence 5' to 3'
SA1-F	GGAGTCCTGATTCGACAGTGT
SA1-R	AACCCGTCAAAAGGGAGATTAC
BLM-F	CAGACTCCGAAGGAAGTTGTATG
BLM-R	TTTGGGGTGGTGTAACAAATGAT
DNA2-F	GGTGCCATACCTGTCACAAAT
DNA2-R	AGGACCGACAAGTTTCTGTCTA
CDKN1C-F	GCGGCGATCAAGAAGCTGT
CDKN1C-R	GCTTGGCGAAGAAATCGGAGA
BRCA1-F	GAAACCGTGCCAAAAGACTTC
BRCA1-R	CCAAGGTTAGAGAGTTGGACAC
CHEK1-F	ATATGAAGCGTGCCGTAGACT
CHEK1-R	TGCCTATGTCTGGCTCTATTCTG
FANCI-F	CCACCTTTGGTCTATCAGCTTC
FANCI-R	CAACATCCAATAGCTCGTCACC
ACTB-F	CATGTACGTTGCTATCCAGGC
ACTB-R	CTCCTTAATGTCACGCACGAT

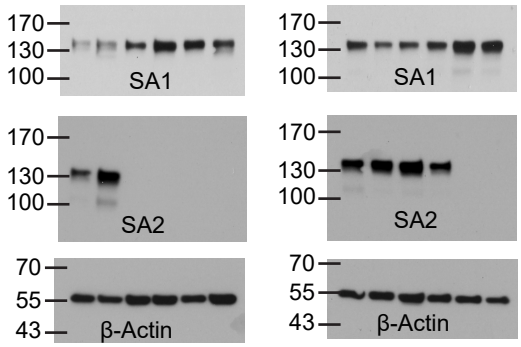

Figure 1F

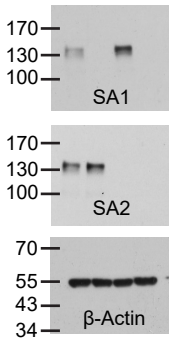

Figure 4F

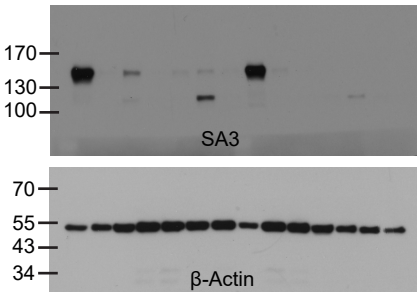

Figure S1E & F

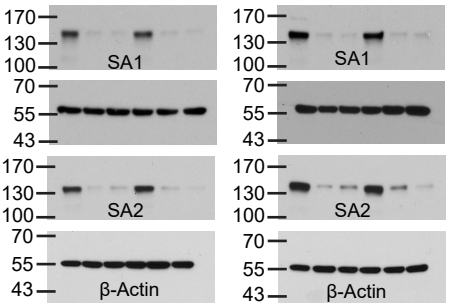

Figure S2A & B

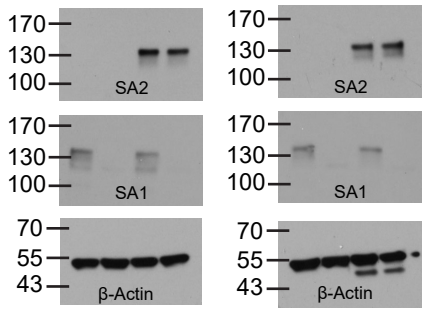

Figure S2E

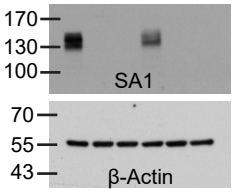

Figure S3D

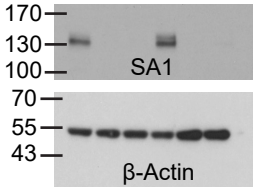

Figure S3G

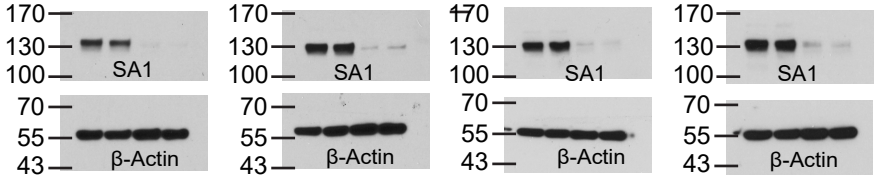

Figure S4F

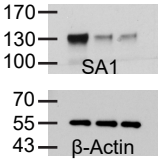

Figure S5C

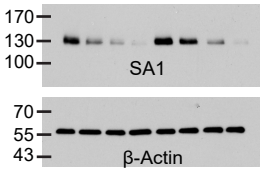

Figure S5E

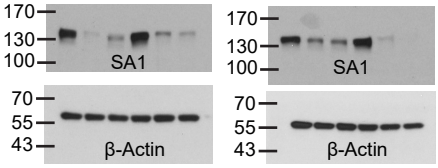

Figure S6C

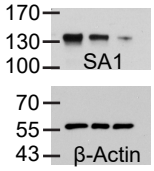

Figure S7E

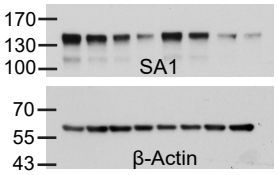

Figure S8C & D

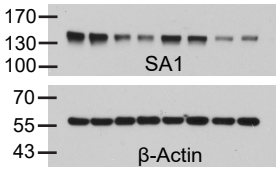

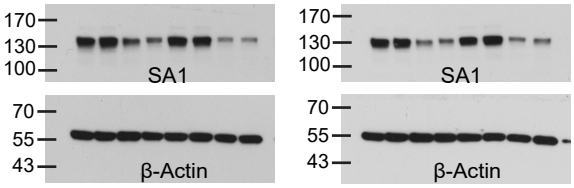

Figure S9G & H